HAGIA SOPHIA IN ISTANBUL: SOME REMARKS ON DISPLACEMENT PHENOMENA IN MAIN PIERS

Gianni Bartoli
Dipartimento di Ingegneria Civile, Università degli Studi di Firenze
via S. Marta, 3 – 50139 Firenze

1. Introduction

The correct understanding of the conservation level of a historical masonry monument often represents a difficult task to deal with, because of both the high number of uncertainties and the difficulties related to the correct representation of the monument's behavior with simple structural schemes.

The nowadays museum of Hagia Sophia (which formerly was a church and a mosque) is one of the most masonry monuments inherited from past days, thus representing an exceptional task for those involved in structural analyses of monumental buildings.

A correct modeling procedure would require, besides the necessary information on the present geometry, the knowledge of all the major steps in the monument's history and evolution; it is then necessary to acquire information about its original shape and the techniques used during its erection, about all the events happened during the life of the monument (collapses and other significant events), about some possible changes in the mechanical behavior (i.e. due to creep or to inelastic deformations). As a matter of facts, the present structural behavior is due to a sequence of events which should be known when dealing with any intervention aimed at the monument's protection.

Some of the aforementioned aspects are enhanced in Hagia Sophia because of the peculiar properties of the masonry which has been used during its erection (very thick mortar beds), because of some important collapses happened during the years, because of a series of substantial interventions aimed to the safeguard of the monument (which often completely modified its structural behavior).

It is then clear then the set-up of a numerical model reproducing the behavior of the whole monument would be almost meaningless, so that in the present study only a particular aspect has been investigated, by using only "partial" structural models.

In Hagia Sophia, one of the most important aspect is represented by the relevant inclination of both main and buttress piers on northern and southern sides of the monument, as it has been reported in other studies performed by Mainstone that will be described in the following [1]. The large difference between the values of dome' main diameters that has been surveyed could then also be due to the "structural weakness" of those structural elements; the analyses of displacements occurred at piers' top level just after their erection will then be the aim of the present research.

After a preliminary section in which some of the most important steps in the history and the evolution of the monument will be sketched, the analysis of piers' displacements will be discussed; the adopted approach consisted in both linear-elastic analyses and nonlinear ones, the latter aimed to define "equivalent" linear parameters to be used in subsequent finite elements models.

2. Some historical notes on erection, collapses and rebuilding

During Nika revolt in January 532 A.D. the existing Hagia Sophia church was fired and partially destroyed. Although most of the brick and stone basilica was probably left standing, Justinian decided to create a new cathedral and the first stone was placed just 40 days after the event. The new church was consecrated on December in the year 537,

that is less than five years were necessary to build the whole monument, essentially the same structure as it stands today.

For more than nine centuries Hagia Sophia represented the masterpiece and the religious center of the Byzantine Empire, the “Megala Ekklesia”; when Constantinople fell to the Ottoman army, 28 May 1453, the young Sultan Mehmet II had the Church of Hagia Sophia turned into his own mosque. Only in 1934 Aya Sofya mosque was opened as a museum and this is its present state.

2.1 Collapses and rebuilding

The global aspect of the building at the time when it was consecrated was certainly different with respect to the present one. The original dome probably presented a different radius of curvature that was the one of a pendentive dome, with the same system of large base ribs and window openings which is clearly visible nowadays; no one of the buttresses and other strengthening works were obviously there.

As it has been reported on some historical documents, at least five different earthquake events hit Constantinople between 542 and 557 A.D. [2]: on December 14th, 557, a severe earthquake caused serious damages to the dome so that some restoration works were planned. During these repairs the eastern semidome, its supporting arch and part of the oriental portion of the dome collapsed, destroying the Lord's Table, the ciborium and the ambo (May 7th, 558).

A complete re-building of the dome and of the eastern semidome was decided, and internal sides of northern and southern arches were corrected (by an increasing change of thickness) in order to give a more circular shape to the impost of the new dome. As a matter of fact North-South and East-West diameters suffered some changes (the former increasing its length and the latter decreasing it) because of the inclination of main piers as well as of the thrusts exerted by the dome. The new dome was rebuilt steeper and of lighter materials.

Successive collapses in 989 and 1346 were very similar to that of 558, and they affected structural western elements and oriental ones respectively. After these two last events, only damaged parts and close structural elements were repaired. At present time, different reconstructions are clearly visible: original portion are the southern and the northern parts, while western has been rebuild after 989 earthquake and eastern after third partial collapse occurred in 1346.

The main western arch is thicker with respect to the original one: it withstood the two earthquakes in 1343 and 1344 that provoked the collapse of the western one, while only small damages occurred during another earthquake in1894.

It is likely that, because of collapses and reconstructions, original structures under the dome level were largely deformed maybe even the 557 event but certainly after the earthquake in 989. As an example, the four towers in which stairs are located turn out to be clearly rotated with respect to main symmetry axes; the rotation, probably due to the horizontal thrusts exerted by the main arches, has been hidden by adding external masonry layers, as recent restoration works put into evidence.

2.2 Additions

Reconstructions altered the original shape of Hagia Sophia, but other three sequences of restoration and strengthening works have been documented through the life of the monument: a first phase begun in 1317 in the reign of Andronicus II Palaeologus; a second one, under the supervision of architect Sinan, started in 1573; a third phase in 1847 due to Swiss architects Giuseppe and Giovanni Fossati. It is just worth to remind that in 1317 the buttresses at the east wall were erected, while Sinan provided for a series of

strengthening works and for the erection of a new minaret. Fossati made some changes at the dome's base level, introduced some steel ties and corrected the verticality of some of the columns in the exedrae.

3. Structural systems in Hagia Sophia

In Hagia Sophia two main structural systems can be observed: referring to Mainstone book [1] and observing the Van Nice surveying [VN], a primary structural system can be identified, which sustains and transfers to lower levels the weight of the superior vaults, while the secondary one is composed by inferior vaults and by the galleries.

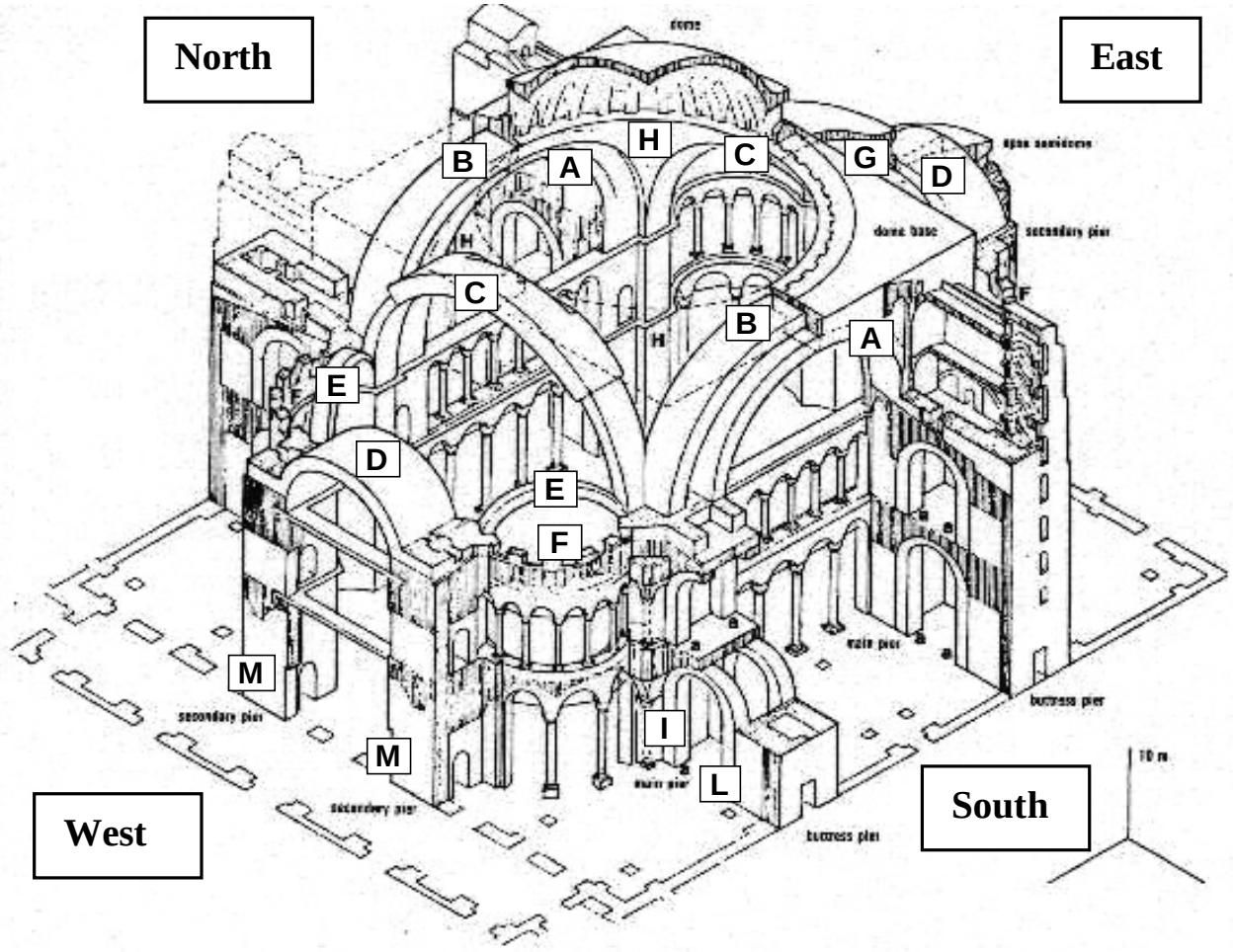

Fig. 1 – The Hagia Sophia primary structural system (Mainstone[1])

A:	*main arches (North and South sides)*	*G:*	*main eastern semidome*
B:	*upper North and South arches*	*H.*	*pendentives*
C:	*main arches (East and West sides)*	*I:*	*main pier*
D:	*East and West barrel vaults*	*L:*	*buttress pier*
E:	*exadrae semidomes arches*	*M:*	*secondary piers*
F:	*exadrae semidomes*		

Both systems border the main space offered by the central aisle and by the background spaces made up by the nartex, the side aisles and the galleries. Starting from the upper level of the monument, the structural restraint to the dome and to the other vaults covering the central aisle is essentially due to main and secondary piers, to buttress piers (all elements are located outside the central aisle) and to the superior arches connecting

them. The primary structural systems we are referring to is then composed by these elements as well as by the dome and the superior vaults.

All the other structural elements constitute the secondary structural system, then consisting of the arches and the vaults of the nartex, of the major halls offered by lateral aisles and of the galleries, besides of their supporting walls and columns not already inserted into the primary system. The secondary system also includes big tympana under North and South main arches and walls around external access ramps. This system is partially supported by the columns surrounding the central aisle and by the main piers of the primary system: a structural dependence of the secondary system from the primary one it is then clear, stating the impossibility of the secondary system of supporting itself without the aid of the other structural system.

The aim of the present work is to focus the structural situation in 535 A.D., in order to understand whether or not the initial configuration of the monument could already be affected by large displacements at the impost level of the dome so that the cross section of the dome could not be perfectly circular even at a very early stage.

In the following, the construction sequence proposed by Mainstone (and nowadays accepted by major scholars) will be adopted in order to give a temporal evolution of the building. In the lack of other information, Mainstone follows the historical sequence of events as it has been reported by the historian at the Court of Justinian, then reconstructing a temporal diagram about the probable evolution of structural works.

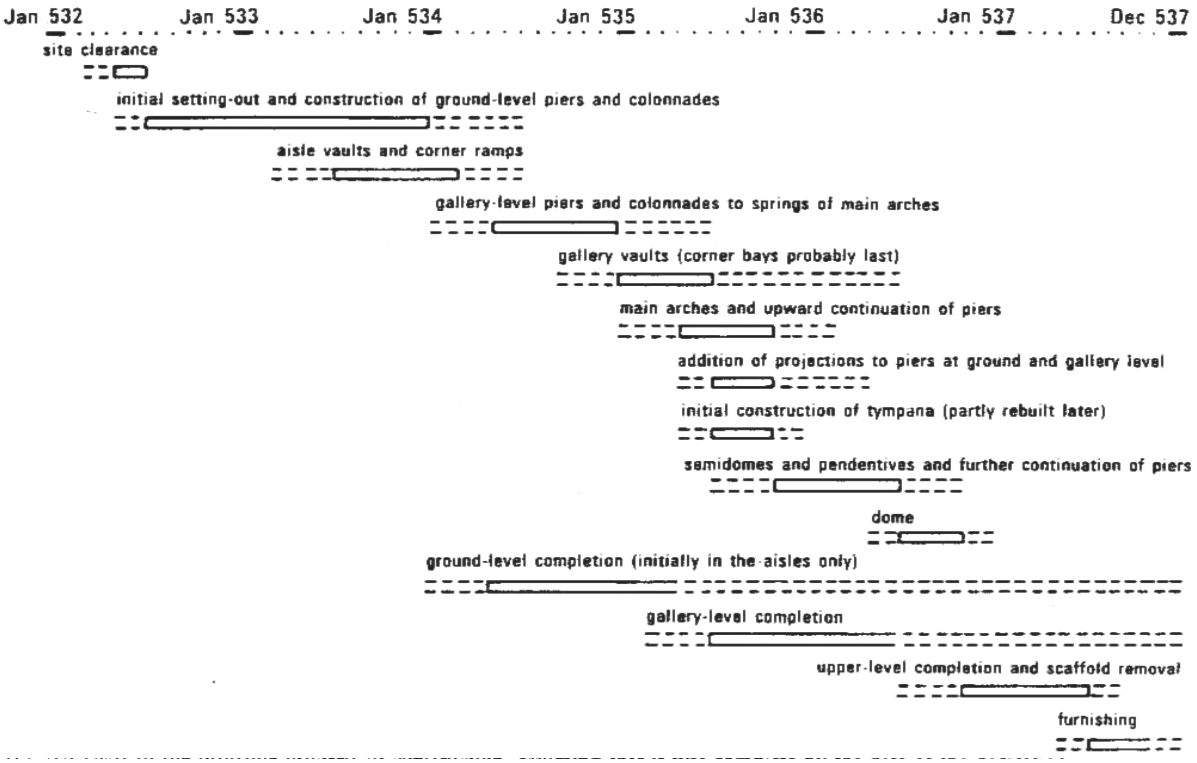

Fig. 2 – Temporal evolution of structural works according to Mainstone [1]

The construction progress of the main structural elements of the monument at the early erection stages can be subdivided into three phases, which are visualized in the following to allow a better understanding of the evolution of such a complex structural system:

phase #1: main piers are built, together with buttress piers, the linking arches and the piers of the secondary system; all structural elements are built from the ground level up to the level of the capitals of aisle's columns.

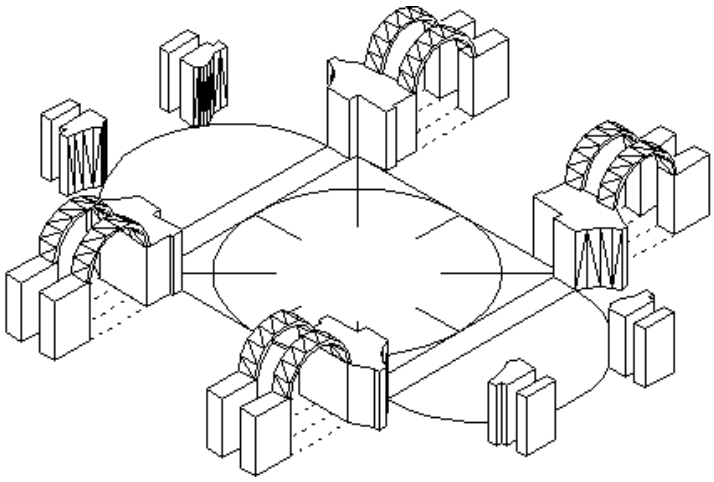

Fig. 3 - Phase #1 of Hagia Sophia erection

phase #2: primary and secondary piers are extended up to second cornice, even if the transversal section is reduced with respect to the lower one. Buttress piers are erected too, but brick masonry is used instead of stone masonry and their building proceeds with increasing speed from the gallery level onward.

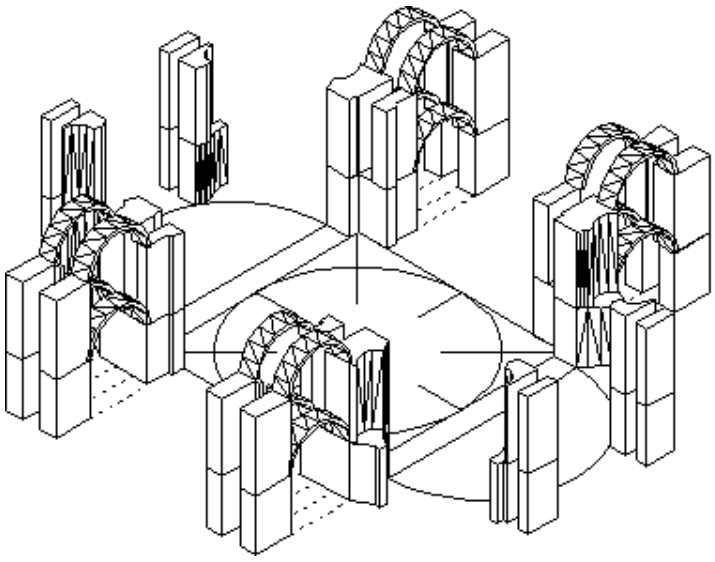

Fig. 4 - Phase #2 of Hagia Sophia erection

phase #3: scaffoldings are taken down from both main and secondary arches restrained by main piers. Horizontal thrusts start to deform piers especially along the North-South direction (due to the thrust exerted by East and West arches) for mainly two reasons: the weakness of the link elements between main and buttress piers, and the differences in elastic moduli and settlements between the two structural elements. Mainstone supposes that self-sustaining centerings have been used in the erection of

minor arches, but he assigns a low probability to the fact that the same system could also be used for main arches; as a matter of fact, self-sustaining centerings are very difficult to be used when dealing with elements possessing large dimensions and, moreover, the presence of other structural elements at lower level could have suggested to adopt usual scaffoldings sustaining the arches during their erection. However, this fact does not necessarily indicate that horizontal thrusts were completely eliminated in the construction phase (as the use of vertical scaffoldings would) as some reported experienced problems during the taking down of the scaffoldings could imply.

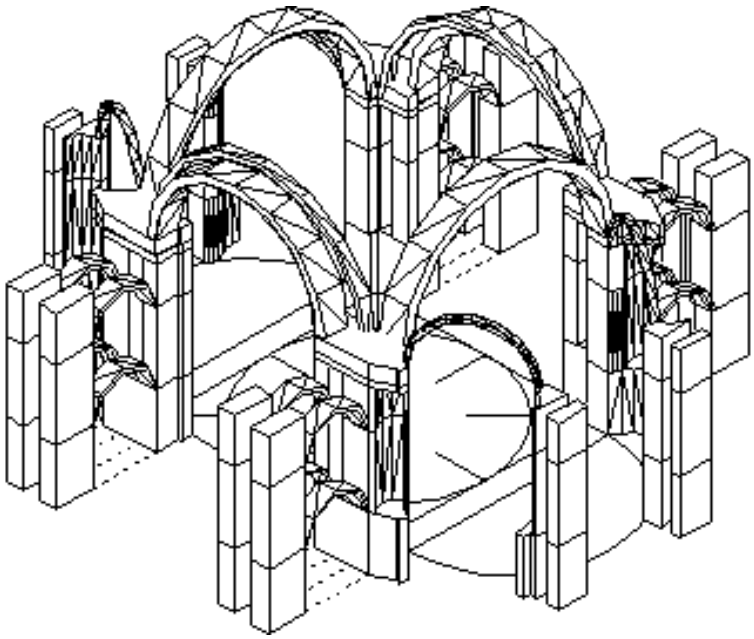

Fig. 5 - Phase #3 of Hagia Sophia erection

3.1 Deformation at the level of dome's impost

Some of major problems which are clearly observable at present time are pointed out by the large difference between diameters at the dome's base level. With respect to the original circular geometry, the theoretical circumference is today deformed and diameters along major monument's axes (North-South and East-West) show very different values.

On the cornice of the present dome two different symmetrical portions can be located (respectively corresponding to South and North side of the dome) which have been built during the first reconstruction in 558; on these sides some reference lines carved on the marble cornice are present and, if one considers these curves as lying on a circular portion, the original radius of curvature can be estimated.

Moreover, the distance between the center of the two circular sectors allows the estimation of the total displacement between the top of the main piers along the North-South direction, due to both the flexural strain of the piers and the movements of the keystone of the main arches under the thrusts of the dome itself.

Mainstone [1] reported the distance between the two centers to a value of 2.83 m; some more recent analyses, after a photogrammetric survey on the monument [H], indicated in 3.338 m the present value of this distance.

Last data processing made by Prof. Kenichiro Hidaka and his co-workers allowed to demonstrate that the curves on the marble exhibit appreciable differences with respect to theoretical circular sectors; this fact, due to evident flexural effects on the arches, leads to

the needing of a new estimation of the distance between centers of the two dome's portions, once flexural effects have been subtracted from. After the new estimation procedure, the distance between the two semicircles can be evaluated in 2.522 ÷ 2.562 m [5], and this value can then be used as a reference value in the following when dealing with the deformation analysis of the main piers.

Half of this value (1.271 m on average) represents the horizontal displacement of the keystone of each of the main arches (North and South sides) with respect to the vertical plane containing them, and without any contribution due to flexural effects induced by the final dome in 562.

Moreover, as it will be shown in following paragraphs when dealing with elastic-linear modeling of the piers, the out-of-plane movement of the arches is roughly the double of the displacement of the top of the main piers. In more details, the keystone of the arch lying in the East-West plane (YZ plane in the following) moves in the X direction (i.e. in the vertical plane containing the North-South direction) by a quantity which is almost twice the movement of the top of the pier.

It is then clear that the displacement between the centers of the two semicircles could be due to a movement of the end-section of the piers only if this movement is equal to half of the value of the global horizontal displacement of the keystone of the arches. Assuming the difference between the two centers equal to 2.542 m (average of the quantities suggested by Prof. Hidaka), the end section of each main pier should exhibit a movement equal to a quarter of this value (about 0.635 m).

According to Mainstone's analysis about the temporal evolution of the deformation (see Fig. 6), about 60% of the total deformation of the piers in the North-South direction should have occurred during the first collapse of the east portion of superior structures in 558. Moreover, Mainstone observed that columns and arches placed as a strengthening of the main piers just after the construction of the two semidomes show an inclination that is roughly equal to 80 ÷ 85 % of the corresponding inclination of piers; is then possible to form the hypothesis that, in the original situation, the inclination of piers was about 15 ÷ 20% of the present one.

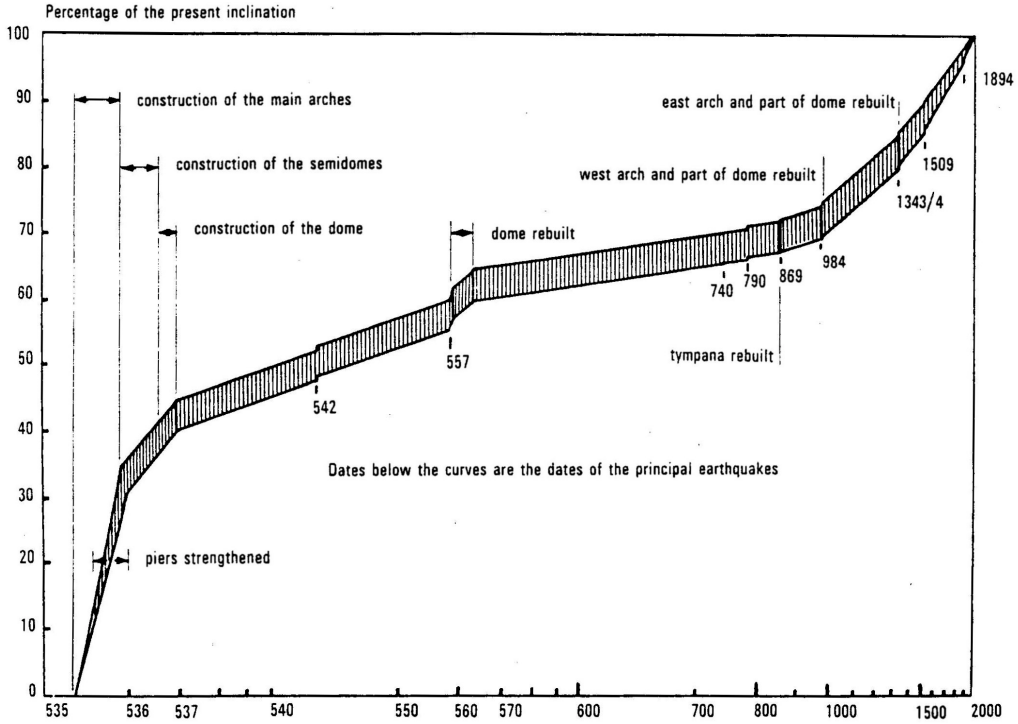

Fig. 6 – Time-evolution of deformations on main piers (after Mainstone, [1])

By the light of previous consideration, displacements of the impost level of the arch in North-South direction (after the scaffoldings were taken down and before the construction of the two semidomes) were in 535 equal to about 0.11 m (15 ÷ 20 % of 0.635 m).

The aim of following sections is then to quantify, by means of as simple as possible analyses, the displacement of the end-section of piers, in order to assess whether or not displacements obtained in an analytical way could justify large values such as those which probably came through at the early phase of the monument's erection.

4. The "pier-system"

According to Mainstone's hypothesis, more representative elements of primary structural system (i.e. piers and their buttress) exhibited their first displacements even during their construction. It is then necessary to focus the attention on these elements in order to quantify movements which could have been occurred at a very early stage of the construction. In the following analyses the attention will then be focused on the "pier-system", that is the system composed by the main piers, their buttress and the linking elements, looking for the evaluation of the tendency of the system to move out of the plane of the main arches after having taken down the scaffoldings.

In the following models only a quarter of the whole structure has been modeled because of the whole symmetry; erection phases are then thought to have progressed symmetrically, as it has been usually assumed. A simplified scheme can be constituted by the "pier-system" as it has been sketched in Fig. 7. The "pier-system" is actually composed by two different systems: the pier and the buttress. It is then necessary to estimate the effectiveness of the linking elements, that is the possibility that forces can be easily transferred between the two sub-systems.

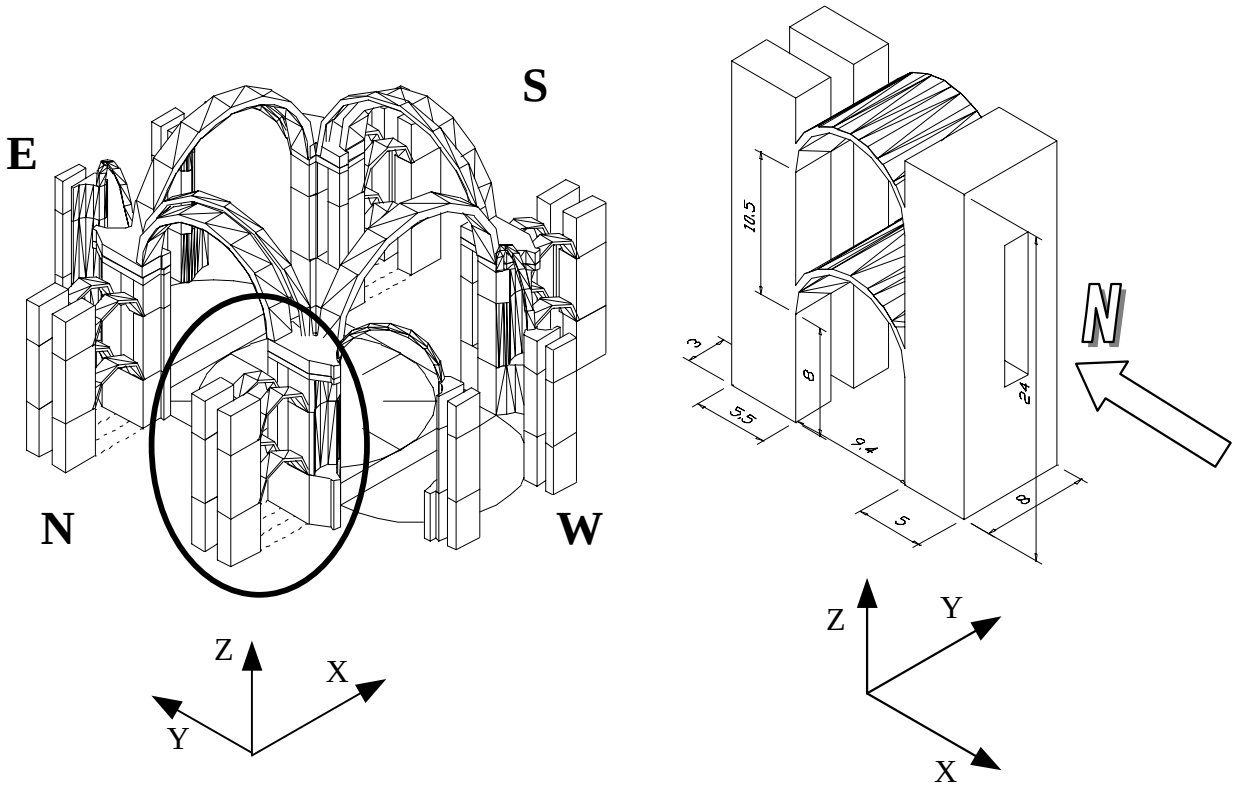

Fig. 7 – The "pier-system" (measures in m)

A linear elastic analysis has been performed by using a Finite Elements Code and by using simple one-dimensional elements (frame elements). The structural components reported in Fig. 7 have been modeled and the analysis pointed out that the whole system behaves essentially as if it were composed by the internal element (pier) only; as reported in Table 1 (where a comparison has been made between the isolated pier and the whole "pier-system"), the effectiveness of the link offered by the arches is very poor, and the only substantial differences arise when considering the behavior along the "strong" axis (i.e. along direction X). In the following, the whole system can then be well represented by the behavior of the internal pier only.

BASE REACTIONS						
	F_X [MN]	F_Y [MN]	F_Z [MN]	M_X [MNm]	M_Y [MNm]	M_Z [MNm]
ISOLATED CANTILEVER						
1) Load –Z + s.w.	0.00	0.00	13.635	0.00	0.00	0.00
2) Load –X	1.00	0.00	0.00	0.00	24.098	0.00
3) Load –Y	0.00	1.00	0.00	-24.097	0.00	0.00
Load combination 1)+2)+3)	*1.00*	*1.00*	*13.635*	*-24.097*	*24.098*	*0.00*
"PIER-SYSTEM"						
1) Load –Z + s.w.	-0.32	0.00	14.547	0.00	-4.296	0.00
2) Load –X	0.94	0.00	0.00	0.00	22.900	0.00
3) Load –Y	0.00	0.97	0.00	-23.309	0.00	0.17
Load combination 1)+2)+3)	*0.63*	*0.97*	*14.542*	*-23.309*	*18.604*	*0.17*
% difference ("pier-system" vs. isolated cantilever)	**63%**	**97%**	**107%**	**97%**	**77%**	**-**

TOP DISPLACEMENTS						
	U_X [cm]	U_Y [cm]	U_Z [cm]	φ_X [mrad]	φ_Y [mrad]	φ_Z [mrad]
ISOLATED CANTILEVER						
Load combination 1)+2)+3)	-1.53	-1.60	-0.122	1.273	1.053	0.000
"PIER-SYSTEM"						
Load combination 1)+2)+3)	-1.29	-1.55	-0.131	1.228	0.916	-0.022
% difference ("pier-system" vs. isolated cantilever)	**84%**	**97%**	**107%**	**96%**	**87%**	**-**

Table 1 – Comparison of base reactions and top displacements between an isolated cantilever (main piers only) and the "pier-system" [applied forces are self weight and concentrated load at top with intensity equal to 1 MN]

5. Numerical modeling

5.1 Problems related with numerical modeling

Mainstone focused one of the possible problems related with Hagia Sophia's construction: the small period of time used for its construction did not allowed the mortar and the bricks to correctly settle, then increasing the deformation of the structure. This aspect can be stressed also due to the fact the Byzantine masonry is composed by mortar joints as thick as the bricks, then leading to an inhomogeneous mechanical behavior.

Several measures have been adopted to control the tendency toward large deformation experienced during the construction of the monument, but they somehow failed, probably because of the time-depending behavior of the masonry (related to creep phenomena).

The aforementioned aspect does not allow to completely characterize the structural behavior of the monument by simply using linear elastic models; on the other hand, the use of complex nonlinear modeling can often lead to misleading results, mainly because of the large amounts of uncertain parameters to be used for a correct modeling of the nonlinear mechanical and time-dependent characteristics.

In the present study, it has been chosen not to increase the complexity of the finite element modeling, then leaving the numerical model as simple as possible and within the limits of a linear-elastic analysis. Non linear aspects have been taken into account by means of simplified models of some structural elements, which have been used to evaluate linear-elastic equivalent properties to be used in the FE models. In following paragraph, some details will be given about the mechanical characterization of the materials adopted in the subsequent analyses.

5.2 Materials parameters

Piers cross section is varying along the height of the pier itself; in the lower part (up to a level of about 18 m) the masonry is made by stones and a filling with cohesive properties, while in the upper part the masonry is simply made by mortar and bricks.

Transversal cross section of piers has been preliminarily brought back to an equivalent rectangular section, as indicated in Fig. 8a, while data derived from literature have been used to characterize the mechanical properties of the masonry.

- ***Stone masonry (lower levels)***

  The thickness of the external layer made by stone masonry is not well known, as well as their mechanical properties and those of the filling material. In the view of looking for the values of the parameters describing the mechanical behavior of an "equivalent" homogenous material, following assumptions have been made.

  As a first approximation, once values for Young's moduli and areas have been chosen for the two materials (E_1 for stone masonry whose area is equal to A_1, E_2 for the filling with area A_2) the "equivalent" Young's modulus can be chosen by imposing vertical displacement equal for the two materials, once a load has been applied. Indicating with N the global vertical force and with N_1 and N_2 the amount of the force on the stone masonry and the filling respectively, the equality of vertical strains implies that

$$\frac{N}{E_{eq} \cdot [A_1 + A_2]} = \frac{N_1}{E_1 \cdot A_1} = \frac{N_2}{E_2 \cdot A_2}$$

  then obtaining

$$N_1 = \frac{N \cdot E_1 \cdot A_1}{E_1 \cdot A_1 + E_2 \cdot A_2} \quad e \quad N_2 = \frac{N \cdot E_2 \cdot A_2}{E_1 \cdot A_1 + E_2 \cdot A_2}$$

The denominator represents the whole stiffness of the cross-section, so that the equivalent modulus can be estimated as

$$E_{eq} = \frac{E_1 \cdot A_1 + E_2 \cdot A_2}{A_1 + A_2}$$

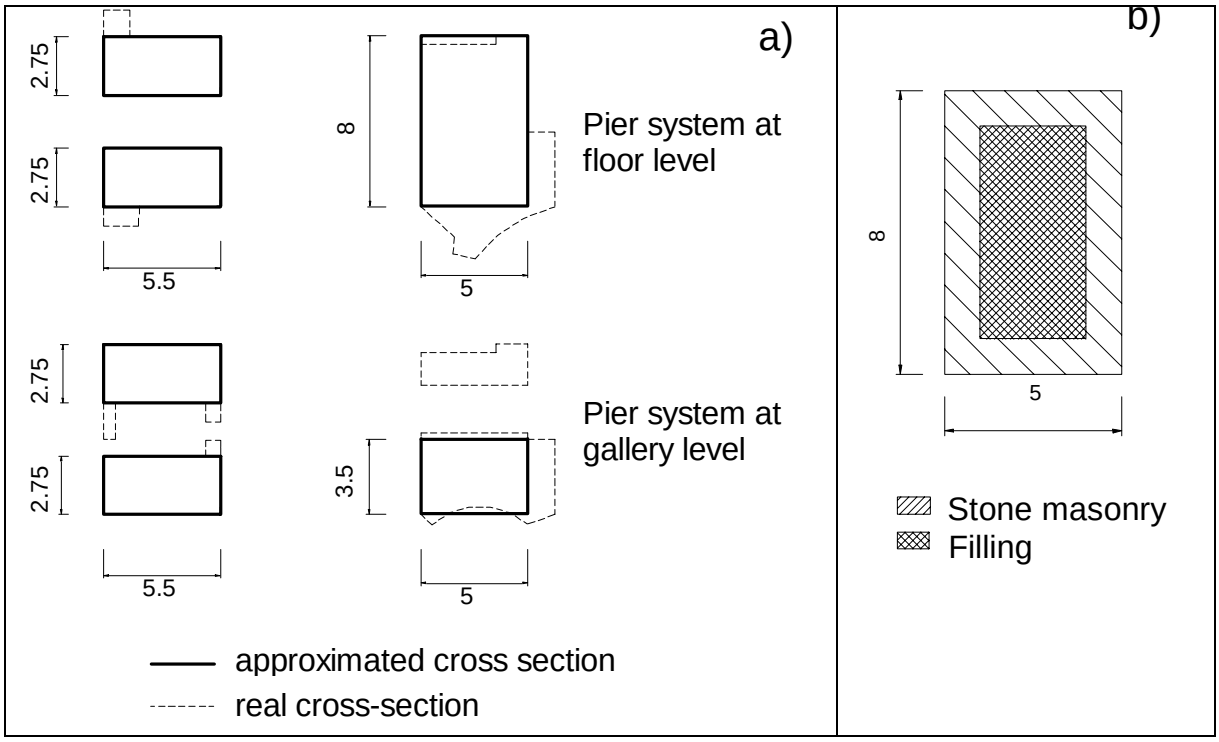

Fig. 9 – Transversal cross-section of the pier (measures in m):
a) geometrical characteristics; b) layers constituting the piers in the lower part

E_{eq} value is then dependent on the ratio between the two areas, the latter depending on the thickness of the external stone layer. By assuming different values for this layer, values reported in Table 2 can be obtained, where E_1=10000 MPa and E_2=2000 MPa have been adopted (according to next Table 3).
Because of the lack of correct information about the effective thickness of the stone layer, a value of E_{eq}=5000 MPa has been chosen in the following, close to the obtained average value.

Stone thickness [m]	E_{eq} [MPa]
0,3	3488
0,6	4832
0,9	6032
average	4784

Table 2 - E_{eq} values as a function of the stone thickness

	Author	Stone masonry	Mortar	Building
Numerical modeling	Croci et al. [6]	10000	2000	Hagia Sophia (Istanbul)
	Hidaka et al. [7]	10000	10000	Hagia Sophia (Istanbul)
Laboratory tests	Penelis, Karaveziroglou [8]	-	2450	Rotunda of Thessa-loniki (early Byzantine age)
	Theocharidou [9]	-	2000	Hagia Sophia in Thessaloniki (beginning of VII century A.D.)

Table 3 – Young's modulus values (in MPa) for different masonry (from cited bibliography)

- ***Stone masonry (upper levels)***

  As a first approach, mechanical characteristics of the masonry composed by alternate mortar and bricks layers with equal thickness could be determined by considering a pure compressive stress state and neglecting all the effects related to strains orthogonal to the direction of the applied force. By utilizing a scheme in which the two different layers can be represented by a series of springs with different characteristics which, under a load P, exhibit a displacement proportional to their stiffness k_1 e k_2 (Fig. 9).
  Being the stiffness of bricks layer higher than the stiffness of mortar layers ($k_1 \gg k_2$), the resulting equivalent stiffness is then

  $K \approx k_2$

  As a consequence, it can be thought that the whole stiffness is governed by the weaker element (the mortar), especially in a first phase when the hardening of the mortar took place.
  According to results reported by recent researches made by the Politecnico di Milano [10], the Young's modulus for the brick masonry can then be assumed equal to the lower value reported in Table 3, that is E_m = 2000 MPa.

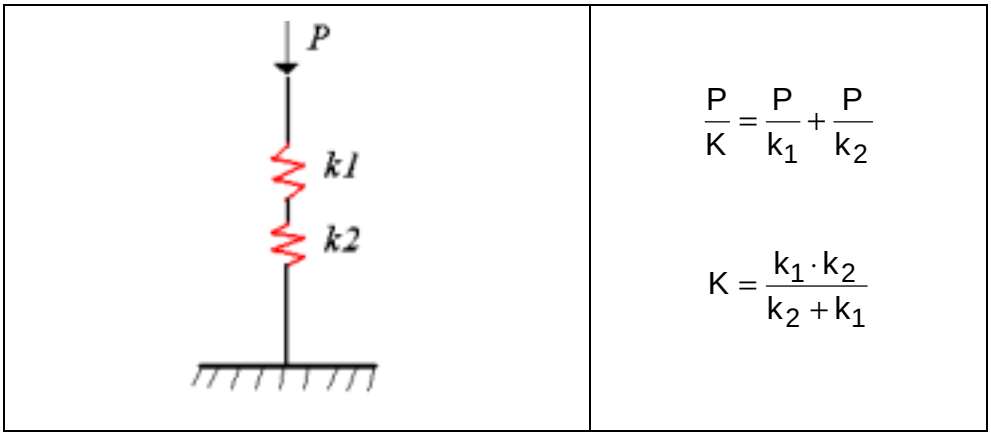

$$\frac{P}{K} = \frac{P}{k_1} + \frac{P}{k_2}$$

$$K = \frac{k_1 \cdot k_2}{k_2 + k_1}$$

Fig. 9 – Series of springs: equivalent stiffness K

5.3 Linear modeling

The characteristics of the materials singled out in previous paragraph can be used for the determination of the stress-strain state in a liner-elastic condition; the analyzed structure is composed by a quarter of the whole structure before the erection of the dome, that is by the "pier-system" and by two semi-arches in the North-South plane (XZ) and in the East-West plane (YZ) respectively. The restraint offered by the external (non modeled) zones has been taken into account by inserting appropriate symmetry restraints.

The portion of the structure has been modeled by using "beam type" elements (see Fig. 10); constituting materials possess the characteristics reported in Table 4. Obtained displacements and internal forces under vertical loads only (self weight) are reported (for the most representative points) in next Table 5.

Parameter	Value
Equivalent Young's modulus for stone masonry	E_s = 5000 MPa
Young's modulus for brick masonry	E_b = 2000 MPa
Poisson coefficient (both materials)	ν=0.3
Specific weight (both materials)	γ=18 kN/m^3

Table 4 – Mechanical characteristics used in the linear elastic models

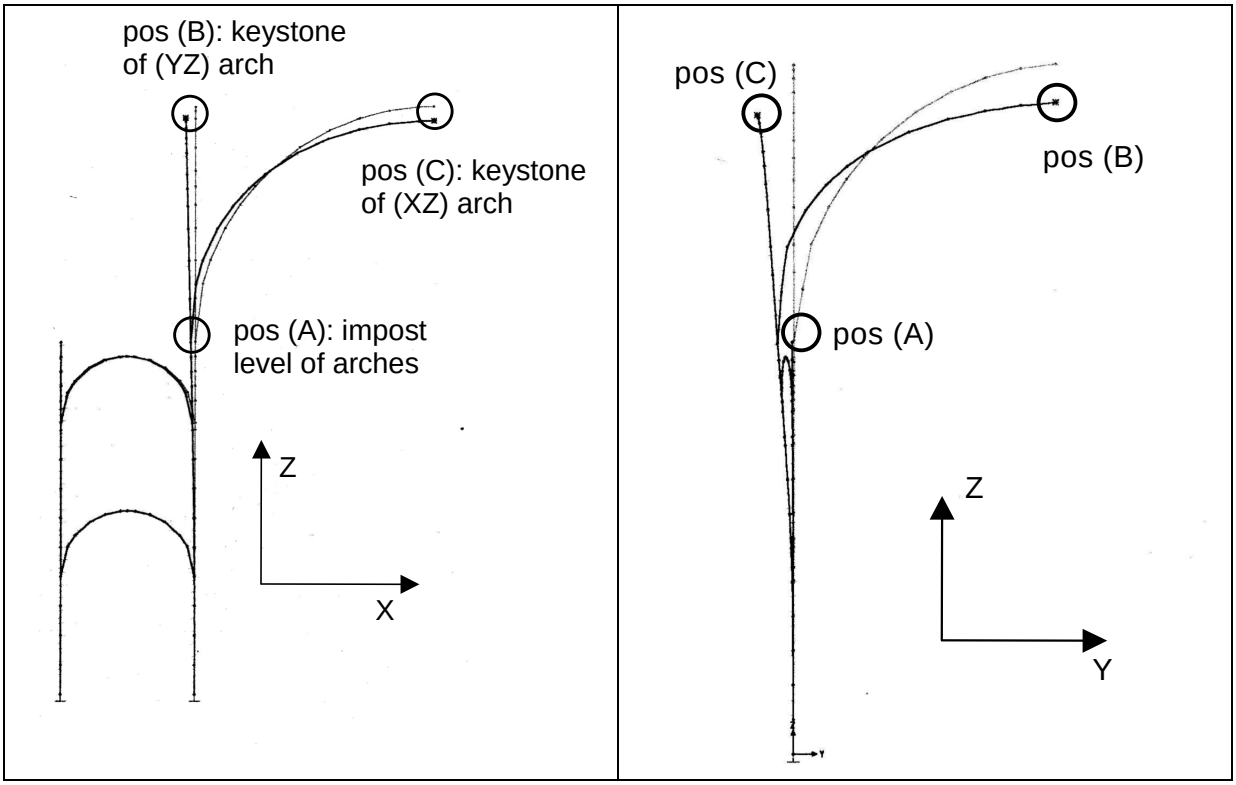

Fig. 10 – Linear elastic model: deformed configuration

5.4 Non linear modeling

In previous paragraph it has been pointed out that the "pier-system" can be adequately schematized by a cantilever constituted by the internal pier only; non-linear calculus can then be carried out for an isolated cantilever element, looking for an extrapolation of information to be used in subsequent analyses.

In following analysis a numerical nonlinear analysis method has been used, based on the one which has been originally set up at the Civil Engineering Department of the University of Florence (Angotti et al. [11]).

By means of the numerical model (see Fig. 11), it is possible to determine the stress-strain state of a slender element under axial and flexural loads, by taking into account different sources of nonlinearities, both geometrical (linked to P-δ effect) and mechanical (nonlinear stress-strain relationships); influence of shear deformation can be taken into account, too.

Displacements	U_X [cm]	U_Y [cm]	U_Z [cm]	φ_X [mrad]	φ_Y [mrad]	φ_Z [mrad]
pos. (A): impost level of arches	-1.58	-1.57	-0.25	1.180	-1.111	-0.033
pos. (B): keystone of (YZ) arch	-3.31	0.00	-3.69	0.000	-1.111	-0.033
pos. (C): keystone of (XZ) arch	0.00	-3.51	-0.48	1.180	0.000	-0.033
Internal forces	F_Z [MN]	F_Z [MN]	F_Z [MN]	M_X [MNm]	M_Y [MNm]	M_Z [MNm]
pos. (A): top level of internal pier	-5.060	-0.999	-0.793	0.737	-1.700	0.000

Table 5 – Results from linear-elastic model (remark: the out-of-plane displacements of keystone points of arches is about the double of the displacement at impost level)

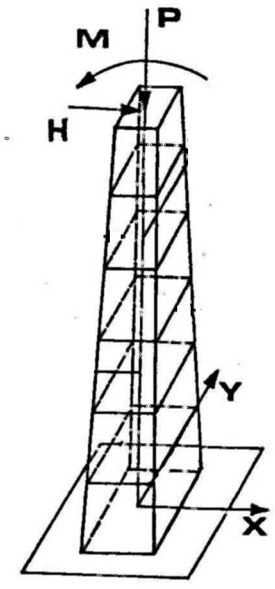

MAIN HYPOTHESES

- Variable section cantilever, with non uniform mechanical properties
- Loads applied at the top level section (in every possible direction) and loading due to self weight
- Finite element discretization of the whole structure
- Cross-section discretization by means of small rectangular elements
- Geometrical nonlinear behavior (P-δ effect)
- Mechanical nonlinear behavior (material with no tensile stresses)
- Shear deformation accounted

Fig. 11 – Nonlinear analysis: reference model and main hypotheses

The adopted makes use of the equations reported in Table 6, where the cantilever with height L is subdivided into n finite elements of equal height $\Delta z=L/n$. The solution procedure is an iterative one: the analysis is stopped when convergence is reached between the stress and the strain state in all the elements.

1) RELATIONSHIP BETWEEN DISPLACEMENTS AND CURVATURES

$$v_1 = \frac{\Delta z^2}{2} \cdot \frac{1}{r_0}$$

$$v_2 = \Delta z^2 \cdot \left[\frac{2}{2r_0} + \frac{1}{r_1} \right]$$

.

$$v_i = \Delta z^2 \cdot \left[\frac{i}{2r_0} + \frac{i-1}{r_1} + \frac{i-2}{r_2} + ... + \frac{2}{r_{i-2}} + \frac{1}{r_{i-1}} \right]$$

.

$$v_n = \Delta z^2 \cdot \left[\frac{n}{2r_0} + \frac{n-1}{r_1} + \frac{n-2}{r_2} + ... + \frac{2}{r_{n-2}} + \frac{1}{r_{n-1}} \right]$$

$$\Delta v_{i,t} = H \cdot \frac{\chi_i}{G \cdot A_i} \cdot z_i$$

v_i: horizontal displacement of i-th finite element (numbering starts from the clamped end)

r_i: radius of curvature of i-th finite element

r_0: radius of curvature of 0-th (base) finite element

$\Delta v_{i,t}$: horizontal displacement of i-th finite element due to shear deformability

z_i: level of i-th finite element

2) RELATIONSHIPS BETWEEN BENDING MOMENTS AND DEFORMED CONFIGURATION

$$M_n = M$$

$$M_{n-1} = M + H \cdot (L - z_{n-1}) + P \cdot (v_n - v_{n-1})$$

.

$$M_i = M + H \cdot (L - z_i) + P \cdot (v_n - v_i) + \sum_{k=i+1}^{n-1} \Delta P_k \cdot (v_k - v_i)$$

$$M_0 = M + H \cdot L + P \cdot v_n + \sum_{k=1}^{n} \Delta P_k \cdot v_k$$

ΔP_i: axial force on i-th finite element

M_i: bending moment at lower level of i-th finite element

M_0: base bending moment (clamped end reaction)

3) GEOMETRICAL CHARACTERISTICS OF RESISTANT SECTION

$$A_c = \int dA \qquad S_x = \int y \, dA$$

$$S_y = \int x \, dA \qquad J_{xy} = \int x \cdot y \, dA$$

$$J_x = \int y^2 \, dA \qquad J_y = \int x^2 \, dA$$

For each finite element the integration domain extends to rectangular elements with negative (compressive) stress

4) RELATIONSHIP BETWEEN INTERNAL FORCES AND CURVATURES

$$E_c \cdot \begin{bmatrix} A_c & S_x & -S_y \\ S_x & J_x & -J_{xy} \\ -S_y & -J_{xy} & J_y \end{bmatrix} \cdot \begin{Bmatrix} \varepsilon_z \\ K_x \\ K_y \end{Bmatrix} = \begin{Bmatrix} N \\ M_x \\ M_y \end{Bmatrix}$$

K_X: curvature in (YZ) plane

K_Y: curvature in (XZ) plane

ε_Z: axial deformation

Table 6 – Main relationships used in the adopted nonlinear calculation

Deformed configuration is defined by means of the centroid displacements in the two planes (XZ) and (YZ), being X and Y the directions corresponding to main inertia axes of the cross-section. Starting from undeformed geometry, the procedure starts by evaluating the values of the internal forces (ensuring global equilibrium through eqn. #2) and then of internal stresses (eqn. #3). New values for internal forces are then evaluated by using the stress-strain relationships (eqn. #4) and hence the displacements (eqn. #1), in both main structural planes. The procedure stops when the obtained stress state and the values of internal forces are in accordance with the strain state and displacement of the centroid of the cross-section.

In the algorithm it is possible to decide whether or not the different sources of nonlinearities have to be taken into account, so estimating the mutual influence among all the different factors involved in the evaluation of the global displacement.

Elastic moduli are the same adopted in the linear-elastic case while for transversal modulus of elasticity G a different value has been used. In order to take into account the high shear deformability due to the thickness of mortar layers, a value equal to G=E/5 has been assumed, then abandoning the linear-elastic relationship.

Loads applied at the end section of the cantilever beam are those derived from linear-elastic calculations performed over a quarter of the whole structure (reported in the last row of previous Table 5).

In the following, main obtained results are reported; Table 7 reports the displacement values at the top level obtained by three different analyses: by considering the no tensile stress condition only, by considering both no tensile stress condition and P-δ effect, and by considering the previous two nonlinear effects plus the shear deformability.

Performed calculation	U_X [cm]	U_Y [cm]	$\sqrt{\left(U_X^2 + U_Y^2\right)}$ [cm]
L) Linear elastic	-1.71	-1.60	2.34
1) No tensile stress condition	-2.85	-2.41	3.73
2) No tensile stress condition + P-δ	-3.47	-2.27	4.15
3) No tensile stress condition + P-δ + shear deformability	-3.71	-2.41	4.42

Table 7 – Displacement at cantilever top level
(E_s=5000 MPa, E_b=2000 MPa)

From reported results it can be noticed that the nonlinear effect giving the highest contribution is the one relate to nonlinear mechanical behavior (absence of tensile resistance); by inserting this effect, displacements increase because of the increased curvature of each single finite element.

The ratio between the top level displacement obtained by the performed nonlinear analysis and the same value when dealing with a linear-elastic calculation is about 2.0. This fact implies that, if one would have only linear-elastic analyses to be performed, different elastic properties of the materials should be adopted with respect to the initial one in order to take (indirectly) into account nonlinear effects. “Correct” moduli values should be as low as 50% of the initial ones, that is equal to

- stone external masonry + filling: E_s = 2500 MPa
- brick masonry: E_b = 1000 MPa

The obtained values for elastic moduli can be used for modeling the elastic behavior of the "pier-system" inserted in the linear elastic model of one quarter of the whole structure, leaving values of elastic moduli of the other structural elements (arches) at the same values as before. Under the same vertical actions, internal forces at the top level of the pier-system are different with respect to those reported in Table 5; by introducing the new obtained top-level forces into the nonlinear procedure sketched before, the new obtained displacement values for the top-level section would be as reported in Table 8.

Performed calculation	U_X [cm]	U_Y [cm]	$\sqrt{\left(U_X^2 + U_Y^2\right)}$ [cm]
1) No tensile stress condition	-1.50	-1.33	2.01
2) No tensile stress condition + P-δ	-2.18	-2.04	2.98
3) No tensile stress condition + P-δ + shear deformability	-2.61	-2.02	3.30

Table 8 – Displacement at cantilever top level
(E_s=2500 MPa, E_b=1000 MPa)

The ratio between the displacement of the top-level of cantilever obtained by a nonlinear analysis and the same quantity obtained by a liner-elastic calculation is now equal to 1.7, so that "correct" values for elastic moduli should be

- stone external masonry + filling: E_s = 2941 MPa
- brick masonry: E_b = 1177 MPa

The procedure should now be repeated until convergence; however, stating the fact the obtained values are intermediate with respect to those initially assumed and those obtained after the first step of this procedure, one would expect that new analyses would lead to top-level displacement values included in the range delimited by previous values, that is to an amplification factor (with respect to linear-elastic modeling) within the range 1.7÷2.0.

As it has been noticed in previous paragraphs, displacement along North-South direction at the impost level of main arches placed in East and West sides of the building should be, after the erection of the two semidomes, as high as about 11 cm in order to justify the measured difference in the main diameters of the dome.

In the reported analyses, performed by using an iterative linear-nonlinear simplified approach, the maximum obtained displacement for the same section (in an erection stage corresponding to the situation immediately before the erection of the two semidomes) can be assumed as within the range 3÷4.5 cm.

6. Concluding remarks

In the present work some initial evaluation of deformation happened in some structural elements during early erection stages of Hagia Sophia have been reported. In more details, the displacements at impost level of the dome have been analyzed by investigating the behavior of main piers, in order to explain the initial "ovalling" tendency in the circular cross-section of the dome.

Calculations have been performed by means of very simple linear models and by iterating a nonlinear procedure based on the behavior of main elements only; the nonlinear analysis shown that simple linear-elastic models could lead to evident underestimation of displacements which have probably occurred in main piers.

The obtained results, however, did not seem to completely justify the actual values which should have occurred in a very early stage of the monument erection. Further analyses will then be performed in order to take into account also viscous phenomena, so to include an effect which probably could lead to more realistic displacements' values, closer to the ones which took place in Hagia Sophia before the erection of the main dome.

7. Acknowledgements

The author wishes to tanks Prof. Kenichiro Hidaka and his co-workers for the support, the help and the advice received during the carrying out of the present research work.

8. References

[1] Mainstone, R.J. (1997). "Hagia Sophia: Architecture, Structure and Liturgy of Justinian's Great Church", Thames & Hudson.

[2] Guidoboni, E. (1994). "Catalogue of ancient earthquakes in the Mediterranean area up to the 10th century", Istituto Nazionale di Geofisica, Roma.

[3] Van Nice, R.L. (1986). "Saint Sophia in Istanbul; an architectural survey", Washington D.C.

[4] Hidaka, K., Sato, T., Kawabe, Y., Yorulmaz, M. (1993). "Photogrammetry of the eastern semi-Dome of Hagia Sophia, Istanbul", Proceedings of the IASS-MSU International Symposium on "Public Assembly Structures from Antiquity to the Present", Istanbul, Turkey, 24-28 May 1993, Ed. Mimar Sinan Universitesi, Istanbul.

[5] Sato, T., Hidaka, K., Kawabe, Y., Aoki, T., Yamashita, K. (1996). "Formal Characteristics of the setting lines on the cornice of the main Dome of Hagia Sophia, Istanbul", J. Arch. Plann. Environ. Eng., Alj, n. 485, July 1996.

[6] Croci, G., Viskovic, A., Nuzzo, M.V. (1995). "Analisi del comportamento strutturale della cupola di S. Sofia ad Istanbul sotto l'effetto dell'azione sismica" (in Italian), Proceedings of 7° Italian Conference on Seismic Engineering "L'ingegneria sismica in Italia", Siena, Italy, 25-28 September 1995.

[7] Kato, S., Aoki, T., Hidaka, K., Nakamura H. (1992). "Finite-element modeling of the first and second domes of Hagia Sophia", in "Hagia Sophia from the Age of Justinian to the Present", edited by R. Mark, A. S. Cakmak, pp. 103-119, Cambridge University Press, USA.

[8] Penelis, G., Karaveziroglou, M., Styliandis, K., Leontaridis D. (1992). "The Rotunda of Thessaloniki: seismic behavior of Roman and Byzantine Structure", in "Hagia Sophia from the Age of Justinian to the Present", edited by R. Mark, A. S. Cakmak, pp. 132-157, Cambridge University Press, USA.

[9] Theocharidou, K. (1992). "The Structure of Hagia Sophia inThessaloniki from its construction to the present", in "Hagia Sophia from the Age of Justinian to the Present", edited by R. Mark, A. S. Cakmak, pp. 83-99, Cambridge University Press, USA.

[10] Binda, L., Tedeschi, C., Baronio, G. (1998). "Mechanical behaviour at different ages of masonry prisms with thick mortar joints reproducing a Byzantine masonry", Politecnico di Milano.

[11] Angotti, F., Chiostrini, S., Vignoli, A. (1988). "Proposta di un metodo numerico per l'analisi di pilastri snelli variamente vincolati" (in Italian), DIC Sezione Strutture n. 2/88, Dipartimento di Ingegneria Civile, Università di Firenze.